Open Access Journal

Journal of Power Technologies 96 (1) (2016) 57–62

journal homepage:papers.itc.pw.edu.pl

Stagnation point flow of Eyring Powell fluid in a vertical cylinder with heat transfer

Abdul Rehman[a,*], Sallahuddin Achakzai[a], Sohail Nadeem[b], Saleem Iqbal[a]

[a] *Department of Mathematics, University of Balochistan, Quetta, Pakistan*
[b] *Department of Mathematics, Quaid-i-Azam University 45320, Islamabad 44000, Pakistan*

Abstract

In this paper an analysis is carried out to examine the effects of natural convection heat transfer for steady boundary layer flow of an Eyring Powell fluid flowing through a vertical circular cylinder. The governing partial differential equations along with the boundary conditions are reduced to dimensionless form by using the boundary layer approximation and applying suitable similarity transformations. The resulting nonlinear coupled system of ordinary differential equations subject to the appropriate boundary conditions is solved using the analytic technique homotopy analysis method (HAM). The effects of the physical parameters on the flow and heat transfer characteristics are presented. The behavior of skinfriction coefficient and Nusselt numbers are also studied for different parameters.

Keywords: Boundary layer flow; Vertical cylinder; Eyring Powell fluid; HAM

1. Introduction

The theory of mixed convection effects comprising temperature difference at different locations of the fluid and heat flow due to some external agent is used widely owing to its important applications in the world of industry and technology. Bachok et al [1] analyzed suction and injection effects on the problem of mixed convection boundary layer steady flow of a viscous fluid over a permeable vertical flat plate embedded in an anisotropic porous medium. In another work, Ahmad et al [2] examined the influence of temperature dependent variable viscosity over the flow of mixed convection boundary layer flow past an isothermal horizontal circular cylinder. Further, Cheng [3] studied the natural convection heat transfer of non-Newtonian fluids in a porous medium from a downward-pointing vertical cone under mixed thermal boundary conditions. Recently, Rashad et al [4] examined the influence of uniform transpiration velocity effects on free convective boundary layer flow of a non-Newtonian fluid over a permeable vertical cone embedded in a porous medium saturated with a nanofluid. In a recent work, Nadeem et al [5] studied the effects of mixed convection heat transfer for the boundary layer flow of a steady viscous nanofluid over a vertical slender cylinder. A few other interesting efforts concerning the concept of mixed convection heat transfer are included in [6–18].

Eyring Powell fluid is a three constant fluid model that is capable of displaying a non-zero bounded viscosity at both the surface of the sheet and the fluid at infinity. Noreen and Nadeem [19] investigated the heat and mass transfer characteristics on the peristaltic flow of an Eyring Powell fluid in an endoscope. In another effort, Yurusoy [20] studied the problem of pressure distribution of a slider bearing lubricated with Eyring Powell fluid. The purpose of the present investigation is to examine the mixed convection heat transfer effects over the steady incompressible flow of Eyring Powell fluids over a vertical circular cylinder. To the best knowledge of the authors the stagnation flow of Eyring Powell fluid in a cylinder has not been explored to date. The solutions of the problem were produced using the homotopy analysis method (HAM). A comparison of the present

*Corresponding author
Email address: rehman_maths@hotmail.com (Abdul Rehman)

solutions is also presented as a special case with the work in [5]. The paper concludes with a results and discussion section that contains a detailed discussion about the physical features the problem entails.

2. Formulation

Consider the problem of mixed convection boundary layer flow of an Eyring Powell fluid through a vertical circular cylinder having radius a The temperature at the surface of the cylinder is assumed to be a constant T_w and the uniform ambient temperature is taken to be T_∞ such that the quantity $T_w - T_\infty > 0$, in the case of the assisting flow, while $T_w - T_\infty < 0$, in case of the opposing flow, respectively. Under the boundary layer assumptions the equations of motion and heat transfer are

$$(rw)_r + ru_x = 0, \tag{1}$$

$$\begin{aligned} &uu_x + wu_r = \_U\frac{dU}{dx} + \nu(1+M)(u_{rr} + \tfrac{1}{r}u_r) - \tfrac{2}{3\rho\beta c^3} \\ &[\tfrac{w^2}{r^2}u_{rr} + u_r(\tfrac{2}{r^2}ww_r - \tfrac{1}{r^3}w + u_x u_{rx} - \tfrac{1}{r}wu_{rx} \\ &-w_{rr}u_{x\_} - w_r u_{rx} - \tfrac{1}{r}w_r u_x) - w_r u_{rr} u_x + \beta^*(T - T_\infty)g], \end{aligned} \tag{2}$$

$$wT_r + uT_x = \alpha(T_{rr} + \frac{1}{r}T_r) + \frac{\nu}{c_p}(1+M)u_r^2 - \frac{4\gamma M}{3c_p c^2}u_r^2(\frac{w^2}{r^2} - w_r u_x), \tag{3}$$

where the velocity components along the $(x,\ r)$ axes are $(w,\ u)$, ρ is density, ν is the kinematic viscosity, p is pressure, c and β are the material fluid parameters, β^* is the coefficient of thermal expansion, g is the gravitational acceleration in x-direction, M is the Eyring Powell parameter, T is the temperature, γ is the curvature parameter, α is the thermal diffusivity, c_p is the specific heat at constant pressure, U_∞ is the surface fluid velocity, and U is the free stream velocity and is defined as $U = U_\infty\left(\frac{x}{l}\right)$.
The corresponding boundary conditions for the problem are

$$u(x,\ a) = 0, \qquad u(x,\ a) \to U(x) \ \text{ as } r \to \infty, \tag{4}$$

$$T(x,\ a) = T_w(x), \quad T(x,\ a) \to T_\infty \text{ as } r \to \infty. \tag{5}$$

3. Solution of the problem

Introduce the following similarity transformations [21]:

$$u = \frac{xU_\infty}{l}f'(\eta), \qquad w = -\frac{a}{r}\left(\frac{\nu U_\infty}{l}\right)^{\frac{1}{2}} f(\eta), \tag{6}$$

$$\theta = \frac{T - T_\infty}{T_w - T_\infty}, \qquad \eta = \frac{r^2 - a^2}{2a}\left(\frac{U_\infty}{\nu l}\right)^{\frac{1}{2}}, \tag{7}$$

where the characteristic temperature ΔT is calculated from the relations $T_w - T_\infty = \left(\frac{x}{l}\right)^2 \Delta T$. With the help of transformations (6) and (7), Eqs. (1) to (3) take the form

$$\begin{aligned} &\_(1+2\gamma\eta)\ f''' + 2\gamma f'' + \tfrac{1}{1+M}(1 + ff'' - f'^2) + \tfrac{KM\gamma}{1+M} \\ &[\left(ff'f''' - f'^2 f''\right) - \gamma(1+2\gamma\eta)\ (3f'f''^2 + f'^2 f''') \\ &-\tfrac{\gamma}{(1+2\gamma\eta)}(ff'f'' + f^2 f''') + \tfrac{2\gamma^2}{(1+2\gamma\eta)^2}f^2 f''] + \lambda\theta = 0, \end{aligned} \tag{8}$$

$$\begin{aligned} &(1+2\gamma\eta)\ \theta'' + 2\gamma\theta' + \Pr(f\theta' - 2f'\theta) + (1+M)\Pr Ec\,(1+2\gamma\eta)\ f''^2 \\ &+2KM\ \Pr\ Ec[\gamma ff'f'' - (1+2\gamma\eta)\ f'^2 f'' - \tfrac{\gamma^2}{(1+2\gamma\eta)}f'^2 f''] = 0, \end{aligned} \tag{9}$$

in which $\gamma = \left(\nu l/U_\infty a^2\right)^{1/2}$, $M = 1/\beta\mu c$, $K = 2U_\infty^2/3c^2l^2$ is the dimensionless Eyring powell parameters, $\lambda = g\beta^*\Delta T x/U_\infty^2$ is the buoyancy parameter, $\Pr = \nu/\alpha$ is the Prandtl number and $Ec = U_\infty^2/c_p\Delta T$ is the Eckert number.
The boundary conditions in nondimensional form are defined as

$$f(0) = b, \quad f'(0) = 0, \quad f' \to 1, \ \text{as } \eta \to \infty, \tag{10}$$

$$\theta(0) = 1, \qquad \theta \to 0, \ \text{as } \eta \to \infty, \tag{11}$$

where b is any constant. The extra boundary condition of $f(0)$ follows from the work in [21].The important associated physical quantities such as shear stress at the surface τ_w, the surface heat flux q_w and the Nusselt numbers Nu are defined as

$$\tau_w = (\tau_{rx})_{r\to a}, \quad q_w = -k(\frac{\partial T}{\partial y})_{y=0}, \quad Nu/Re_x^{1/2} = -\theta'(0), \tag{12}$$

where τ_{rx} is the component of stress tensor, k is the thermal conductivity and Re_x is the local Reynolds number.

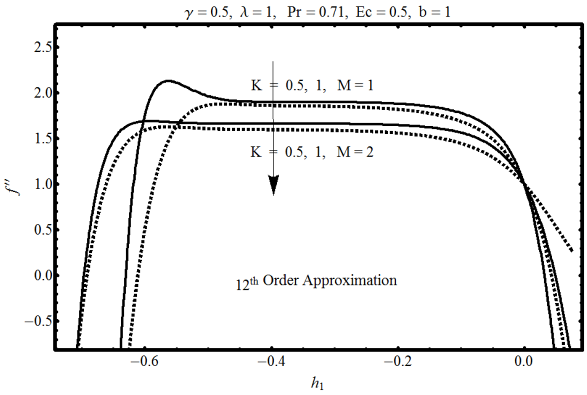

Figure 1: $\hbar_1$—curves for f' plotted for different values of K and M

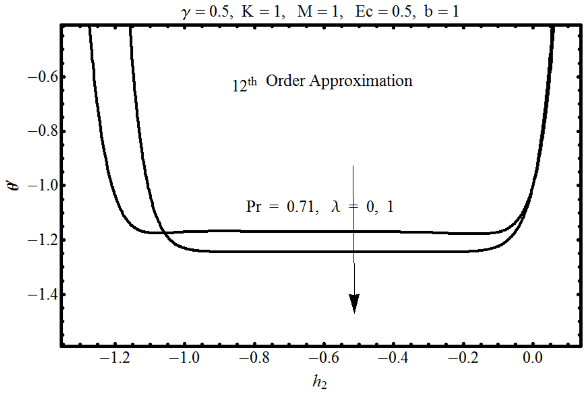

Figure 2: $\hbar_2$—curves for θ plotted for different values of Pr and λ

The solution of the present problem is obtained by using the powerful analytical technique homotopy analysis method (HAM). In the present case we seek initial guesses to be [19, 20, 22–30]

$$f_0(\eta) = b - 1 + \eta + e^{-\eta}, \qquad \theta_0(\eta) = e^{-\eta}. \tag{13}$$

The corresponding auxiliary linear operators are

$$L_f = \frac{d^3}{d\eta^3} + \frac{d^2}{d\eta^2}, \qquad L_\theta = \frac{d^2}{d\eta^2} + \frac{d}{d\eta}, \tag{14}$$

satisfying

$$L_f[c_1 + c_2\eta + c_3 e^{-\eta}] = 0, \quad L_\theta[c_4 + c_5 e^{-\eta}] = 0, \tag{15}$$

where $c_i\,(i = 1, ..., 5)$ are arbitrary constants. The zeroth-order deformation equations are

$$(1-q)\; L_f[\hat{f}(\eta;q) - f_0(\eta)] = \_qH_f\hbar_1 N_f[\hat{f}(\eta;q)], \tag{16}$$

$$(1-q)\; L_\theta[\hat{\theta}(\eta;q) - \theta_0(\eta)] = \_qH_\theta\hbar_2 N_\theta[\hat{\theta}(\eta;q)], \tag{17}$$

where the auxiliary convergence parameters H_f and H_θ, both are taken to be $e^{-\eta}$.

Further details of the HAM procedure can be found in the listed references. However, the numerical results of the present solutions are presented in the proceeding section.

4. Results and discussion

The problem of steady incompressible flow of non-Newtonain Eyring Powell fluid flowing through a vertical circular cylinder under the influence of mixed convection heat transfer and deceptions effects is computed by applying the powerful analytic technique homotopy analysis method (HAM). An associated fact with the HAM solutions is their dependence upon the auxiliary convergence parameters $\hbar_1$ and $\hbar_2$ corresponding to momentum and heat transfer, respectively. Figs. 1 and 2 are included to observe the convergence region of the involved auxiliary parameters for different combinations of other involved parameters. Fig. 1 shows the acceptable convergence regions computed at the surface of the sheet, for the auxiliary parameter $\hbar_1$ for different combinations of K and M when the bouncy parameter $\lambda = 1$ and the deception rate Eckert number $Ec = 0.5$. It is noticed from Fig. 1 that with increase in K, the convergence region decreases, whereas the acceptable region for $\hbar_1$ is greater for $M = 2$ than for $M = 1$. The convergence region for velocity profile with $K = 1$, $M = 1$ is $-0.5 \le \hbar_1 \le -0.1$. Fig. 2 is included to observe the convergence region for the auxiliary parameter $\hbar_2$ involved in heat transfer for different values of bouncy parameter λ, when $\mathrm{Pr} = 0.71$. It is noted from Fig. 2 that the convergence region with $\lambda = 0$ is greater than for non-zero λ. Specifically for $\lambda = 0$ the convergence region is $-1.1 \le \hbar_2 \le -0.1$.

The influence of different involved parameters over the heat and fluid flow are presented in Figs. 3 to 8. Figs. 3 to 5 are displaying the effects of some involved parameters over the fluid flow while Figs. 6 to 8 are drafted to observe the influence of different parameters over the heat transfer characteristics. Fig. 3 is prepared to predict the influence of curvature parameter γ and Eyring Powell fluid parameter M over the nondimensional velocity profile for presented values of the other involved parameters. From Fig. 3 it is observed that with increase in both γ and M the velocity profile decreases.

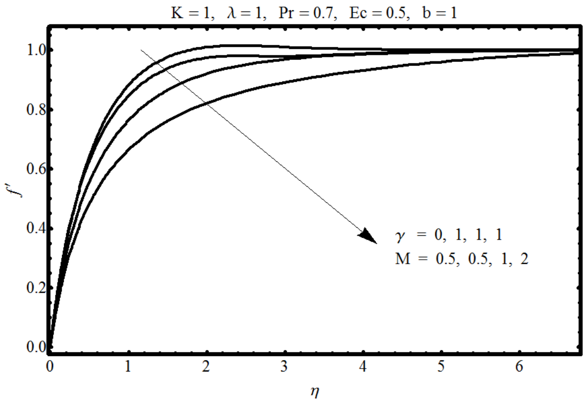

Figure 3: Influence of γ and M over f'

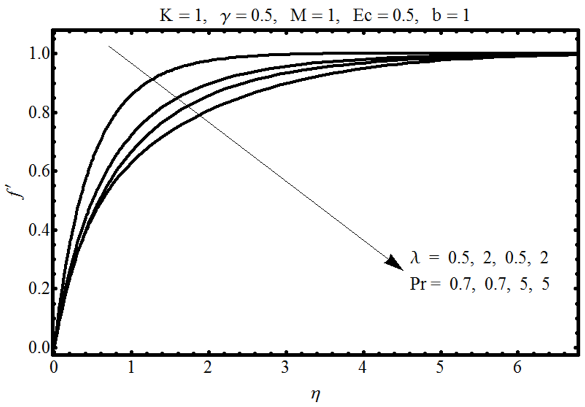

Figure 4: Influence of λ and Pr over f'

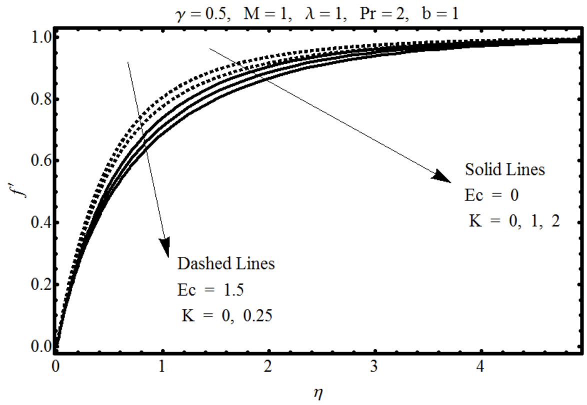

Figure 5: Influence of K and Ec over f'

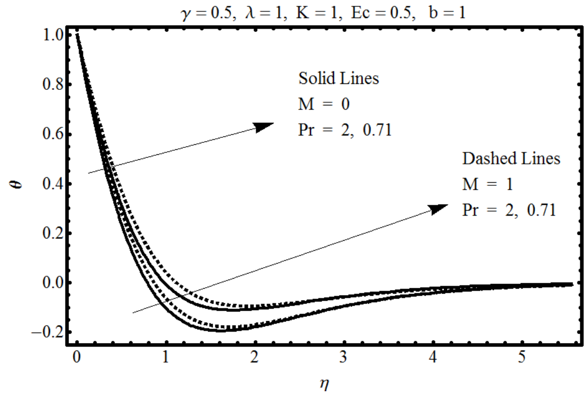

Figure 6: Influence of Pr and M over θ

Fig. 4 depicts the pattern adopted by the velocity profile f' for different combinations of buoyancy parameter λ and Prandtl number Pr for Eyring Powell fluids with $K = 1$ and $M = 1$. From this sketch it is noted that with increase in both λ and Pr, the velocity profile and momentum boundary layer thickness decreases. The behavior of different Eyring Powell parameter K and the Eckert number Ec over the velocity profile f' is presented in Fig. 5. From Fig. 5 it is noticed that with increase in K the velocity profile decreases while with increase in Ec, the velocity profile increases.

The behavior of temperature profile θ for different values of Prandtl number Pr and Eyring Powell parameter M is portrayed in Fig. 6. From Fig. 6 it is obvious that with increase in Pr the temperature profile θ decreases while with increase in M the temperature profile θ increases. Fig. 7 gives the influence of curvature parameter γ and Prandtl number Pr over the temperature profile θ. From Fig. 7 it is observed that with increase in both Pr and γ the temperature profile decreases. Fig. 8 is included to observe the influence of K and Ec over the temperature profile θ. From this figure it is clear that with increase in K, the temperature profile θ decreases while with increase in Ec the temperature profile enhances.

Fig. 9 exhibits the influence of Reynolds numbers Re over the skinfriction coefficient c_f Plotted against the Eyring Powell parameter K. From this sketch it is evident that for smaller K, increase in Re decreases the skinfriction coefficient c_f, while for larger K increase in Re increases c_f. Fig. 10 gives the impact of Prandtl numbers Pr over the local Nusselt numbers Nu graphed against the Reynolds numbers Re. From Fig. 10 it is clear that with increase in both Pr and Re the local Nusselt numbers increases.

Table 1 gives a comparison of the special case of the present solutions with the existing work [5]. From Table 1 it is noted that the two results are in excellent agreement. Table 2 contains the values of velocity boundary derivatives corresponding to the shear stress at the surface of the cylinder tabulated for different combinations of Eyring Powell parameters K and Eckert numbers Ec, whereas Table 3 is prepared for values of the temperature boundary derivatives corresponding

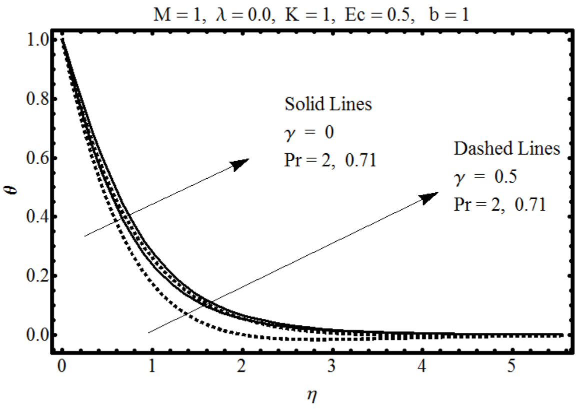

Figure 7: Influence of Pr and γ over θ

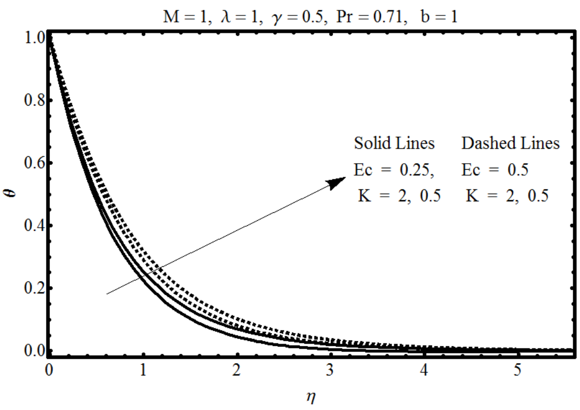

Figure 8: Influence of Ec and K over θ

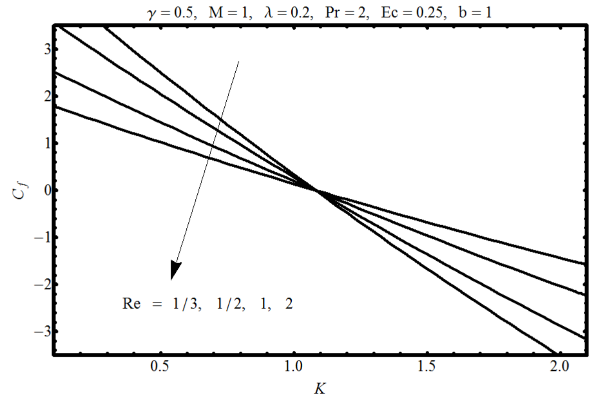

Figure 9: Influence of Re over c_f against K

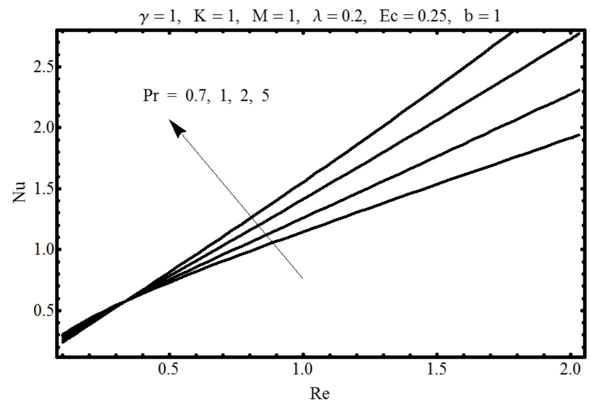

Figure 10: Influence of Pr over Nu against Re

to heat flux at the surface of the cylinder for different Prandtl numbers Pr and Eyring Powell parameter M. From Table 2 it is noticed that with increase in Ec, shear stress at the surface increases for small K, while the surface shear stress decreases for larger K. From Table 3 it is deduced that with increase in Pr heat flux at the surface of the cylinder increases whereas with increase in M heat flux at the surface of the cylinder decreases.

Table 1: Comparison of boundary derivatives for velocity profile of present results with [5] for various values of b and γ when $\lambda = 0$ and $M = 0$

	f"(0)					
	[5]	Present	[5]	Present	[5]	Present
b\γ	0.5		1.0		1.5	
-1	0.9918	0.9918	1.1942	1.1942	1.3729	1.3729
0	1.4886	1.4886	1.7244	1.7244	1.7954	1.7954
1	2.0397	2.0397	2.1751	2.1751	2.2982	2.2982
2	2.7332	2.7332	2.8029	2.8029	2.8746	2.8746

References

[1] N. Bachok, A. Ishak, I. Pop, Mixed convection boundary layer flow over a permeable vertical flat plate embedded in an anisotropic porous medium, Mathematical Problems in Engineering 2010.

[2] S. Ahmad, N. M. Arifin, R. Nazar, I. Pop, Mixed convection boundary layer flow past an isothermal horizontal circular cylinder with temperature-dependent viscosity, International Journal of Thermal Sciences 48 (10) (2009) 1943–1948.

[3] C.-Y. Cheng, Natural convection heat transfer of non-newtonian fluids in porous media from a vertical cone under mixed thermal boundary conditions, International Communications in Heat and Mass Transfer 36 (7) (2009) 693–697.

Table 2: Influence of boundary derivatives of velocity profile computed for different K and Ec when $\gamma = 1/2$, $\lambda = 1$, $M = 1$, $\Pr = 2$, $b = 1$

	f"(0)			
$K \backslash Ec$	0.0	0.5	1.0	2.0
0.25	1.64972	1.70540	1.76175	1.87704
0.5	1.64217	1.678150	1.71382	1.78499
1.0	1.63028	1.62787	1.62154	1.59678
1.5	1.62251	1.58337	1.53498	1.41169
2.0	1.61867	1.54481	1.45576	1.23916

Table 3: Influence of boundary derivatives for temperature profile computed for different Pr and M when $\gamma = 1/2$, $\lambda = 1$, $K = 1$, $Ec = 1/2$, $b = 1$

	$\Theta'(0)$					
Pr\M	0.0	0.2	0.5	1.0	1.5	2.0
0.2	0.804943	0.797271	0.790688	0.786252	0.785742	0.768891
0.7	1.41593	1.38826	1.36393	1.34629	1.34239	1.32229
2.0	2.86071	2.77536	2.69642	2.63032	2.60349	2.5963
5.0	5.40207	5.15247	4.90081	4.64499	4.48737	4.37883
7.0	6.4818	6.09855	5.6955	5.25285	4.94765	4.71118
10.0	7.17962	6.55968	5.87522	5.40583	5.18915	4.87365

[4] A. Rashad, M. El-Hakiem, M. Abdou, Natural convection boundary layer of a non-newtonian fluid about a permeable vertical cone embedded in a porous medium saturated with a nanofluid, Computers & Mathematics with Applications 62 (8) (2011) 3140–3151.

[5] S. Nadeem, A. Rehman, M. E. Ali, The boundary layer flow and heat transfer of a nanofluid over a vertical, slender cylinder, Proceedings of the Institution of Mechanical Engineers, Part N: Journal of Nanoengineering and Nanosystems (2012) 1740349912453806.

[6] C.-L. Chang, Buoyancy and wall conduction effects on forced convection of micropolar fluid flow along a vertical slender hollow circular cylinder, International journal of heat and mass transfer 49 (25) (2006) 4932–4942.

[7] A. Rehman, S. Nadeem, Heat transfer analysis of the boundary layer flow over a vertical exponentially stretching cylinder, Global J. Sci. Fron. Res 13 (11) (2013) 73–85.

[8] A. Rehman, S. Nadeem, S. Iqbal, M. Y. Malik, M. Naseer, Nanoparticle effect over the boundary layer flow over an exponentially stretching cylinder, Proceedings of the Institution of Mechanical Engineers, Part N: Journal of Nanoengineering and Nanosystems (2014) 1740349913517872.

[9] M. Malik, M. Naseer, S. Nadeem, A. Rehman, The boundary layer flow of casson nanofluid over a vertical exponentially stretching cylinder, Applied Nanoscience 4 (7) (2014) 869–873.

[10] C.-Y. Cheng, Natural convection boundary layer on a horizontal elliptical cylinder with constant heat flux and internal heat generation, International Communications in Heat and Mass Transfer 36 (10) (2009) 1025–1029.

[11] A. Rehman, S. Nadeem, Mixed convection heat transfer in micropolar nanofluid over a vertical slender cylinder, Chinese Physics Letters 29 (12) (2012) 124701.

[12] M. Naseer, M. Y. Malik, S. Nadeem, A. Rehman, The boundary layer flow of hyperbolic tangent fluid over a vertical exponentially stretching cylinder, Alexandria engineering journal 53 (3) (2014) 747–750.

[13] J.-M. Buchlin, Natural and forced convective heat transfer on slender cylinders, Revue générale de Thermique 37 (8) (1998) 653–660.

[14] A. Mahdy, F. Hady, Effect of thermophoretic particle deposition in non-newtonian free convection flow over a vertical plate with magnetic field effect, Journal of Non-Newtonian Fluid Mechanics 161 (1) (2009) 37–41.

[15] M. Naseer, M. Malik, A. Rehman, Numerical study of convective heat transfer on the power law fluid over a vertical exponentially stretching cylinder, Applied and Computational Mathematics 4 (5) (2015) 346–350.

[16] A. Rehman, R. Bazai, S. Achakzai, S. Iqbal, M. Naseer, Boundary layer flow and heat transfer of micropolar fluid over a vertical exponentially stretched cylinder, Applied and Computational Mathematics 4 (6) (2015) 424–430.

[17] A. Rehman, G. Farooq, I. Ahmed, M. Naseer, M. Zulfiqar, Boundary layer stagnation-point flow of second grade fluid over an exponentially stretching sheet, American Journal of Applied Mathematics and Statistics 3 (6) (2015) 211–219.

[18] A. Rehman, S. Nadeem, M. Malik, Stagnation flow of couple stress nanofluid over an exponentially stretching sheet through a porous medium, Journal of Power Technologies 93 (2) (2013) 122–132.

[19] S. Nadeem, A. Rehman, Axisymmetric stagnation flow of a nanofluid in a moving cylinder, Computational mathematics and modeling 24 (2) (2013) 293–306.

[20] M. Yurusoy, A study of pressure distribution of a slider bearing lubricated with powell-eyring fluid., Turkish Journal of Engineering and Environmental Sciences 27 (5) (2003) 299–304.

[21] A. Ishak, R. Nazar, I. Pop, The effects of transpiration on the boundary layer flow and heat transfer over a vertical slender cylinder, International Journal of Non-Linear Mechanics 42 (8) (2007) 1010–1017.

[22] S. Nadeem, A. Rehman, K. Vajravelu, J. Lee, C. Lee, Axisymmetric stagnation flow of a micropolar nanofluid in a moving cylinder, Mathematical Problems in Engineering 2012.

[23] A. Rehman, S. Nadeem, M. Malik, Boundary layer stagnation-point flow of a third grade fluid over an exponentially stretching sheet, Brazilian Journal of Chemical Engineering 30 (3) (2013) 611–618.

[24] S. Liao, Beyond perturbation: introduction to the homotopy analysis method, CRC press, 2003.

[25] R. Ellahi, A. Zeeshan, K. Vafai, H. U. Rahman, Series solutions for magnetohydrodynamic flow of non-newtonian nanofluid and heat transfer in coaxial porous cylinder with slip conditions, Proceedings of the Institution of Mechanical Engineers, Part N: Journal of Nanoengineering and Nanosystems (2011) 1740349911429759.

[26] S. J. Liao, An approximate solution technique which does not depend upon small parameters:a special example, International Journal of Non-Linear Mechanics 30 (3) (1995) 371–380.

[27] A. Alomari, M. Noorani, R. Nazar, On the homotopy analysis method for the exact solutions of helmholtz equation, Chaos, Solitons & Fractals 41 (4) (2009) 1873–1879.

[28] S. Nadeem, A. Rehman, C. Lee, J. Lee, Boundary layer flow of second grade fluid in a cylinder with heat transfer, Mathematical Problems in Engineering 2012.

[29] S. Abbasbandy, The application of homotopy analysis method to nonlinear equations arising in heat transfer, Physics Letters A 360 (1) (2006) 109–113.

[30] A. Alomari, M. Noorani, R. Nazar, Explicit series solutions of some linear and nonlinear schrodinger equations via the homotopy analysis method, Communications in Nonlinear Science and Numerical Simulation 14 (4) (2009) 1196–1207.